Thermomechanical Continuum Interpretation of Atomistic Deformation

*Min Zhou**

George W. Woodruff School of Mechanical Engineering
Georgia Institute of Technology
Atlanta, GA 30332-0405

ABSTRACT

This paper describes a framework for obtaining thermomechanical continuum interpretations of the results of molecular dynamics calculations. This theory is a further advancement from a pure mechanical equivalent continuum theory developed recently. The analysis is based on the decomposition of atomic particle velocity into a structural deformation part and a thermal oscillation part. On one hand, balance of momentum at the structural level yields fields of stress, body force, traction, mass density, and deformation as they appear to a macroscopic observer. The full dynamic equivalence between the discrete system and continuum system includes (i) preservation of linear and angular momenta; (ii) conservation of internal, external, and inertial work rates; and (iii) conservation of mass. On the other hand, balance of momentum for the thermal motions as it appears to an observer moving at the structural velocity yields the fields of heat flux and temperature. These quantities can be cast in a manner as to conform to the continuum phenomenological equation for heat conduction and generation, yielding scale-sensitive characterizations of specific heat, thermal conductivity, and thermal relaxation time. The coupling between the structural deformation and the thermal conduction processes results from the fact that the equations for structural deformation and for heat conduction are two different forms of the same balance of momentum equation at the fully time-resolved atomic level. This coupling occurs through an inertial force term in each of the two equations, induced by the other process. For the structural deformation equation, the inertial force term induced by thermal oscillations of atoms gives rise to the phenomenological dependence of deformation on temperature. For the heat equation, the inertial force term induced by structural deformation takes the phenomenological form of a heat source.

*Address all correspondence to min.zhou@me.gatech.edu

1. INTRODUCTION

Although molecular dynamics (MD) theories provide explicit resolution of particle motions and structures of atomic systems, continuum theories provide approximate characterizations of the atomic events and atomic structural states in an aggregate sense. Continuum models often have far fewer numbers of degrees of freedom (DOF) than MD models. At the atomic level, structural deformation and thermal fluctuation make up the total atomic motion. MD models explicitly track the total displacement. Continuum theories, however, treat these two parts of atomic motion separately and, to a degree, independently. Specifically, although the structural deformation part is explicitly modeled at the continuum level, the thermal oscillation part is only accounted for phenomenologically, in the form of heat energy. Reconciliation of the differences in the two descriptions and, more importantly, the integration of the two frameworks of analyses for cross-scale characterization are a great challenge in physics, material science, and mechanics. Statistical mechanics is an important theoretical approach in this endeavor. This approach, however, does not maintain strict fidelity to molecular processes. For example, statistical mechanics characterizations do not resolve deformation mechanisms associated with dislocations at the nanoscale. They cannot be used to analyze the generation and reaction of dislocations and other defects. Since they do not resolve nonlocal interactions and discreteness- and nonlocality-induced length scales, they are not suitable for analyzing nanoscale processes. Ultimately, in the context of multiscale modeling and characterization of material behavior "from the ground up" (from *ab initio*, first principle, MD, to micro-, meso-, and macroscopic continuum models), the formulation of continuum descriptions from the results of MD simulations must be carried out with a high degree of faithfulness. As an important first step, the continuumization of atomic descriptions should maintain time-resolved equivalence in momentum, work rates, mass, and kinetic energy. The nonlocality of atomic interactions and discreteness- and nonlocality-induced length scales must be described in the continuum representation. Also, the thermal oscillation part and the structural deformation part of the atomic motion must be delineated as one approaches higher length scales. Other issues include scaling, reduction of number of degrees of freedom, and extraction of phenomenological quantities.

An equivalent continuum (EC) representation has recently been developed for discrete atomistic systems under conditions of general dynamic deformation. A polar version of this theory is given in [1] for particle systems exhibiting moment interactions as well as central force interactions. A nonpolar version of this theory is given in [2] for systems with only central force interactions. This new theoretical framework uses an explicit expression of all atomic degrees of freedom. Not only are work-conjugate continuum stress and deformation fields defined, but also specified are all other work- and momentum-preserving kinetic quantities and mass distributions for the equivalent continuum. The continuum is equivalent to its corresponding MD system in that, at all times, it preserves the linear and angular momenta of the particle system, it conserves the internal and external mechanical work rates, and it has an equal amount of kinetic energy and contains the same amount of mass as the particle system. The EC is a fully dynamic representation of the MD system rather than a less rigorous, lower-order thermodynamic representation. The equivalence between the discrete system and EC holds for the entire system and for volume elements defined by any subset of particles in the system; therefore, averaging and characterization across different length scales

are possible and size-scale effects can be explicitly analyzed. The development of the EC uses the fact that discrete atomistic and continuum theories are based on the same fundamental laws, including Newton's laws of motion, conservation of energy, and conservation of mass. This equivalent continuum theory is a nanoscale mechanical theory. Just like in the MD system represented by the EC, the kinetic energy of the EC includes both the thermal part and the structural dynamic part. In this sense, the EC is a fully faithful continuum form representation of the MD model. By faithful here, we mean time-resolved, explicit equivalence in all work rates, kinetic energy, mass, and deformation fields. Just like MD models explicitly track the absolute particle motion and the total kinetic energy, the EC model does the same by explicitly following the motion of the particles in a fully time-resolved manner. The EC development can be and, perhaps, should be regarded as the continuumization of discrete models that offers a high degree of fidelity to the discrete description. Following this initial step, further development could involve scaling in time and space. In this paper, the EC theory is extended to account for the thermal and mechanical processes at continuum scales. The new thermomechanical equivalent continuum (TMEC) theory described herein allows scale-dependent continuum descriptions of material behavior in the form of coupled thermomechanical processes of deformation and heat conduction to be obtained from molecular dynamics simulations at the atomic level.

2. THERMOMECHANICAL EQUIVALENT CONTINUUM

2.1 Two Perspectives of Particle System Deformation

Consider a dynamically deforming system of N particles that occupies space V and has an

envelope of surface S, as shown in Fig. 1. At time t, particle i has position $\mathbf{r}_i$, displacement $\mathbf{u}_i$, and velocity $\dot{\mathbf{r}}_i = \dot{\mathbf{u}}_i$. $\dot{\mathbf{r}}_i = \mathrm{d}\mathbf{r}_i/\mathrm{d}t$ denotes the material time derivative. The interparticle force applied on particle i by particle j is $\boldsymbol{f}_{ij}(\mathbf{r}_{ij})$ where $r_{ij} = |\mathbf{r}_{ij}| = |\mathbf{r}_j - \mathbf{r}_i|$ is the central distance between particle i and particle j. Note that Newton's third law requires that $\boldsymbol{f}_{ij} = -\boldsymbol{f}_{ji}$. This analysis here admits pairwise Lennard-Jones type potentials and multibody interactions models such as the embedded atom method (EAM) potential [3], the modified EAM potentials [4,5], and other potentials [6,7].

In most cases, however, the high-frequency (thermal) part of the atomic velocity cannot be or is not explicitly resolved. Instead, the thermal oscillation part is phenomenologically accounted for as heat in continuum theories. This is both convenient and necessary in most microscopic and macroscopic theories. In order to admit such an analysis in the EC theory and allow a transition to higher-scale continuum theories, a thermomechanical equivalent continuum (TMEC) theory is developed in this section. To this objective, a decomposition of the atomic displacement $\mathbf{u}_i$ into a structural deformation part $\bar{\mathbf{u}}_i$ and a thermal oscillation part
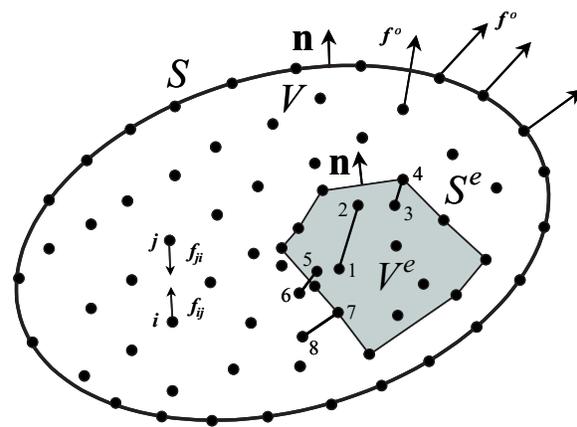

FIGURE 1. Particle system and equivalent continuum at arbitrary size scale

$\tilde{\mathbf{u}}_i$ is considered. Based on this decomposition, a thermomechanical version of the equivalent continuum theory is developed. The structural-thermal decomposition can be written as

$$\mathbf{u}_i = \bar{\mathbf{u}}_i + \tilde{\mathbf{u}}_i \tag{1}$$

The fact that $\tilde{\mathbf{u}}_i$ is the high-frequency part and $\bar{\mathbf{u}}_i$ is the relatively "slowly" changing part dictates that the decomposition be carried out with regard to the time evolution of $\mathbf{u}_i$ and not be solely accomplished in a spatial manner without regard to time history. This decomposition is dependent on both the size scale and time scale of the analysis pursued. Therefore, there is no unique demarcation between the two parts that can be universally applied under all scales. However, some basic features of the decomposition can be outlined. Specifically, this division can be obtained through a Fourier analysis in time or in both time and space. This may be accomplished, for example, by obtaining a spectral representation of $\dot{u}_i$ in the form of

$$\vartheta_i(\nu) = \frac{1}{\sqrt{2\pi}} \int\limits_{-\infty}^{\infty} \dot{\mathbf{u}}(t) e^{\hat{i}\nu t} \mathrm{d}t$$

$$= \bar{\vartheta}_i(\nu) + \tilde{\vartheta}_i(\nu); \text{ where}$$

$$\bar{\vartheta}_i(\nu) = \begin{cases} \vartheta_i(\nu), & \text{if } \nu < \nu_{\text{cutoff}} \\ 0, & \text{if } \nu \geq \nu_{\text{cutoff}} \end{cases} \text{ and}$$

$$\tilde{\vartheta}_i(\nu) = \begin{cases} 0, & \text{if } \nu < \nu_{\text{cutoff}} \\ \vartheta_i(\nu), & \text{if } \nu \geq \nu_{\text{cutoff}} \end{cases}$$

$$(2)$$

In the above expressions, $\hat{i} = \sqrt{-1}$, ν is frequency, and ν_{cutoff} is a cutoff frequency whose choice depends on the time and size scales of analysis. Since thermal oscillations are typically at frequencies in the range of 0.5–50 THz [8] and structural deformation occurs at much lower frequencies, ν_{cutoff} can be unambiguously determined. Inverse transforms would yield the structural and the thermal velocities, i.e.,

$$\dot{\bar{\mathbf{u}}}_i(t) = \frac{1}{\sqrt{2\pi}} \int\limits_{-\infty}^{\infty} \bar{\vartheta}_i(\nu) e^{-\hat{i}\nu t} \mathrm{d}\nu \text{ and}$$

$$\dot{\tilde{\mathbf{u}}}_i(t) = \frac{1}{\sqrt{2\pi}} \int\limits_{-\infty}^{\infty} \tilde{\vartheta}_i(\nu) e^{-\hat{i}\nu t} \mathrm{d}\nu$$

$$(3)$$

The spectral analysis outlined here is, perhaps, only one out of many possible approaches for decomposition. Even though the analysis is carried out for each atom separately in a purely temporal manner, it can allow the spatial propagation of lattice waves at different frequencies to be revealed. This is simply because the spatial distribution of the structural part of atomic motions is represented in $\mathbf{u}_i$ for each atom.

We note that thermal oscillations are usually associated with no net momentum at the system level. Specifically,

$$\sum_{i=1}^{N} m_i \tilde{\mathbf{u}}_i = \mathbf{0}, \ \sum_{i=1}^{N} m_i \dot{\tilde{\mathbf{u}}}_i = \mathbf{0}, \text{ and } \sum_{i=1}^{N} m_i \ddot{\tilde{\mathbf{u}}}_i = \mathbf{0} \quad (4)$$

Under the decomposition in Eq. (1), the position of particle i can be written as

$$\mathbf{r}_i = \bar{\mathbf{r}}_i + \tilde{\mathbf{u}}_i \tag{5}$$

This decomposition of atomic positions defines the difference between the *actual configuration* (V^e and S^e) and the *macroscopically perceived* configuration ($\bar{V}^e$ and $\bar{S}^e$) of an arbitrary volume element. An illustration of the macroscopically perceived configuration and the actual configuration is given in Fig. 2. Although the pure mechanical EC theory in Refs. [1] and [2] is formulated over the actual configuration, the thermal mechanical equivalent continuum (TMEC) here must be formulated over the macroscopically perceived configuration.

The force on particle i due to atoms or agents that are *external* to the system under consideration is $\boldsymbol{f}_i^o$. The total force on i is

FIGURE 2. Actual and macroscopically perceived configurations

$$f_i = \sum_j f_{ij} + f_i^o = f_i^{\text{int}} + f_i^{\text{ext}} \qquad (6)$$

Here, the summation is over those particles inside the system of N particles that interact directly with particle i. It is worthwhile to point out that due to nonlocal interactions, external force can exist for particles both in the interior of V and on surface S. Note that the concepts of internal and external forces are specific to the particular subvolume V^e of V considered. So, in general, $f_i^{\text{int}} \neq \sum_j f_{ij}$ and $f_i^{\text{ext}} \neq f_i^o$, except for $V^e = V$. For example, for the volume element V^e illustrated in Fig. 1, the forces between atoms 1 and 2 (f_{12}, f_{21}) as well as those between atoms 3 and 4 (f_{34}, f_{43}) are internal; whereas the forces between atoms 5 and 6 (f_{56}, f_{65}) and those between atoms 7 and 8 (f_{78}, f_{87}) are external. Note that all these forces are internal when the system is considered as a whole.

Note that balance of momentum must be satisfied by a system as a whole and by any portion of the system. For a given portion of a system, internal forces and external forces are fundamentally different and play different roles. Therefore, if two systems are to be equivalent

and the balance of momentum is to be satisfied at any size scale, their internal force work rate, external force work rate, and inertial work rate at all size scales must be equivalent.

To develop a scalable representation of the equivalent continuum, consider a subvolume element $V^e \subset V$ with closed surface S^e associated with a subset of $M (\leq N)$ particles in the ensemble. Assume that M_S out of the M particles ($M_S \leq M$) are on surface S^e, therefore defining it. The remaining $M - M_S$ particles are in the interior of V^e and are considered as internal particles for V^e.

The equation of motion for an atom is

$$f_i^{\text{int}} + f_i^{\text{ext}} = m_i \left(\ddot{\bar{\mathbf{u}}}_i + \ddot{\tilde{\mathbf{u}}}_i \right) \qquad (7)$$

There are two distinctive yet related perspectives toward this equation. These two aspects can be illustrated using two different observers. An illustration of this issue is given in Fig. 3. The first observer is stationary and has a macroscopic resolution for atomic motion. This observer uses a slower-responding oscilloscope that is insensitive to motions at frequencies above ν_{cutoff}. Consequently, $\tilde{\mathbf{u}}_i$ is not explicitly resolved or is "invisible" at the size and time scales analyzed by this macroscopic observer. To understand the motion as it appears to the macroscopic observer, we rewrite Eq. (7) as

$$f_i^{\text{int}} + f_i^{\text{ext}} + \left(-m_i \ddot{\tilde{\mathbf{u}}}_i \right) = f_i^{\text{int}} + f_i^{\text{ext}} + \widehat{f}_i = m_i \ddot{\bar{\mathbf{u}}}_i \quad (8)$$

where $\widehat{f}_i$ is the high-frequency inertial force $-m_i \ddot{\tilde{\mathbf{u}}}_i$. Since $\ddot{\tilde{\mathbf{u}}}_i$ is not directly measurable for the macroscopic observer, $\widehat{f}_i$ is not directly measurable. The macroscopically observed trajectory is $\bar{\mathbf{r}}_i(t) = \mathbf{r}_{i0} + \bar{\mathbf{u}}_i(t)$ (see Fig. 3).

However, the observer can "feel" the effect of $\widehat{f}_i$ or infer its existence from the deviation of
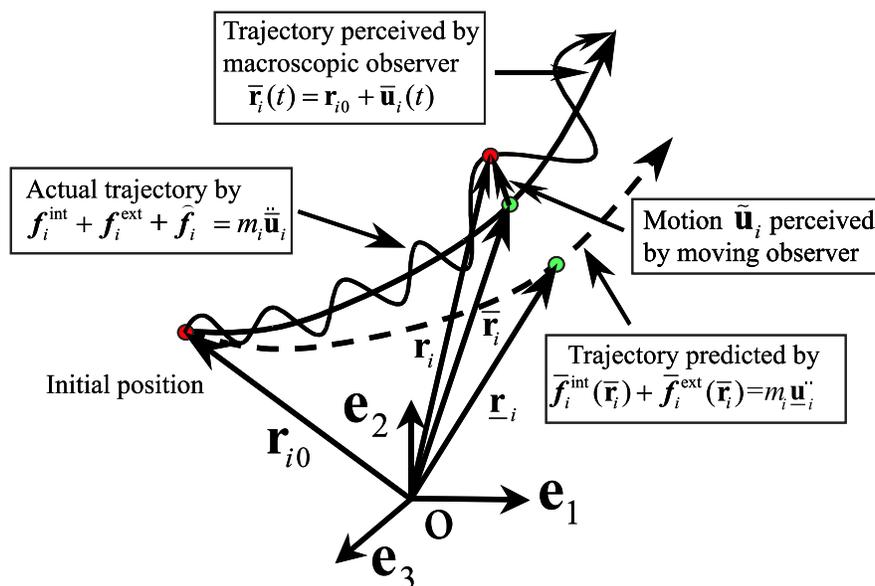
FIGURE 3. Actual, macroscopically perceived, and macroscopically predicted trajectories for an atomic particle

the average path $\bar{\mathbf{r}}_i(t)$ (which he or she actually measures) from what is predicted by

$$\bar{\boldsymbol{f}}_i^{\text{int}}(\bar{\mathbf{r}}_i) + \bar{\boldsymbol{f}}_i^{\text{ext}}(\bar{\mathbf{r}}_i) = m_i \ddot{\underline{\mathbf{u}}}_i \qquad (9)$$

This equation consists of only kinetic and kinematic quantities perceivable to the observer. In particular, $\bar{\boldsymbol{f}}_i^{\text{int}}(\bar{\mathbf{r}}_i)$ and $\bar{\boldsymbol{f}}_i^{\text{ext}}(\bar{\mathbf{r}}_i)$ are "slowly-varying" forces evaluated using the macroscopically observed positions $\bar{\mathbf{r}}_i$; in contrast, $\boldsymbol{f}_i^{\text{int}}(\mathbf{r}_i)$ and $\boldsymbol{f}_i^{\text{ext}}(\mathbf{r}_i)$ are actual forces evaluated using the actual positions $\bar{\mathbf{r}}_i$. Equation (9) describes the trajectory if thermal oscillations simply do not occur ($\tilde{\mathbf{u}}_i = \mathbf{0}$ at all times). We must note that, although $\bar{\mathbf{r}}_i(t)$ describes the "perceived" deformation and Eq. (9) defines the "macroscopically predicted" deformation of an atomic system at longer time and higher size scales, it is Eq. (8) that governs the actual deformation on which the "perception" is based. The perceived state $\bar{\mathbf{r}}_i(t)$ is important since it defines the volume $\bar{V}^e$ and surface $\bar{S}^e$ that form the configura-

tion required by a macroscopic analysis. The analysis of macroscopic deformation (balance of momentum and balance of energy), however, must use Eq. (8).

The second perspective toward Eq. (7) is based on the observation of an observer traveling with the structural velocity $\dot{\bar{\mathbf{u}}}_i$ of an atom. Assume that this observer uses an oscilloscope that can resolve motions at all frequencies. To this observer, the particle motion then appears to be governed by

$$\boldsymbol{f}_i^{\text{int}} + \boldsymbol{f}_i^{\text{ext}} + (-m_i \ddot{\bar{\mathbf{u}}}_i) = \boldsymbol{f}_i^{\text{int}} + \boldsymbol{f}_i^{\text{ext}} + \breve{\boldsymbol{f}}_i = m_i \ddot{\tilde{\mathbf{u}}}_i \quad (10)$$

where $\breve{\boldsymbol{f}}_i$ is the inertial force $-m_i \ddot{\bar{\mathbf{u}}}_i$ due to the structural deformation. Compared to $\widehat{\boldsymbol{f}}_i$, $\breve{\boldsymbol{f}}_i$ is slow-changing. Since $\ddot{\bar{\mathbf{u}}}_i$ is invisible to this moving observer, he can only infer the effect (and, therefore, the existence) of $\breve{\boldsymbol{f}}_i$ by noting the deviation of $\tilde{\mathbf{u}}_i$ from what is predicted by

$$\tilde{\boldsymbol{f}}_i^{\text{int}}(\mathbf{r}_{i0} + \tilde{\mathbf{u}}_i) + \tilde{\boldsymbol{f}}_i^{\text{ext}}(\mathbf{r}_{i0} + \tilde{\mathbf{u}}_i) = m_i \ddot{\tilde{\mathbf{u}}}_i \quad (11)$$

In the above equation, $\tilde{\boldsymbol{f}}_i^{\text{int}}$ and $\tilde{\boldsymbol{f}}_i^{\text{ext}}$ are, respectively, the internal and external forces on atom i calculated using the atomic position $(\mathbf{r}_{i0} + \tilde{\mathbf{u}}_i)$ as perceived by the observer moving with $\bar{\mathbf{u}}_i$. $\ddot{\tilde{\mathbf{u}}}_i$ represents the solution to the above equation which in general differs from the displacement solutions to Eqs. (7-10). Equation (11) consists of only kinetic and kinematic quantities perceivable to the moving observer. It describes the trajectory of the thermal oscillations if the structural deformation simply did not occur ($\bar{\mathbf{u}}_i = 0$ at all times). It is important to point out that, just like Eq. (9), Eq. (11) is cited here for comparison and perspective only. It is not used to develop any equation of consequence in this paper.

It will become clear later that Eqs. (8) and (10) govern, respectively, the macroscopically observed deformation and the thermal behavior of a material system. These two equations yield the coupled mechanical and thermal equations at various scales, respectively. We will also see that the inertial forces $\widehat{\boldsymbol{f}}_i$ and $\widecheck{\boldsymbol{f}}_i$ give rise to the coupling between the mechanical and the thermal processes. The fact that Eq. (10) is written from the perspective of an observer moving with a particle's macroscopic velocity $\dot{\bar{\mathbf{u}}}_i$ indicates that heat conduction analyzed here is relative to material mass at the macroscopically perceived positions $\bar{\mathbf{r}}_i$. Therefore, a material time derivative should be used later in the continuum representation of internal energy. This also requires the heat flux to be defined relative to macroscopically perceived, current, atomic positions $\bar{\mathbf{r}}_i$ (as opposed to $\mathbf{r}_i$ or $\mathbf{r}_{i0}$).

2.2 Structural Deformation: Balance Laws and Field Quantities

To analyze the behavior of the system associated with macroscopically observable struc-tural deformation $\bar{\mathbf{u}}_i$, we consider a variation of this velocity ($\delta\dot{\bar{\mathbf{u}}}_i$) and invoke the principle of virtual work for an arbitrary element *as it appears to the macroscopic observer*. Under this condition, the equivalence can be stated as

$$\sum_{I=1}^{M} \boldsymbol{f}_I^{\text{int}} \cdot \delta\dot{\mathbf{u}}_I + \sum_{I=1}^{M}\left(\boldsymbol{f}_I^{\text{ext}} + \widehat{\boldsymbol{f}}_I\right)\cdot\delta\dot{\mathbf{u}}_I$$
$$+ \sum_{I=1}^{M_S}(1 - \kappa_I)\boldsymbol{f}_I^{\text{ext}}\cdot\delta\dot{\mathbf{u}}_I = \sum_{I=1}^{M}\bar{\varsigma}_I m_I \ddot{\mathbf{u}}_I\cdot\delta\dot{\mathbf{u}}_I$$
$$= -\int_{\bar{V}^e}\bar{\boldsymbol{\sigma}}^{(e)}:\delta\bar{\mathbf{D}}^{(e)}\mathrm{d}\bar{V} + \int_{\bar{V}^e}\left(\bar{\boldsymbol{b}}^{(e)} + \widehat{\boldsymbol{b}}^{(e)}\right)\cdot\delta\dot{\mathbf{u}}^{(e)}\mathrm{d}\bar{V}$$
$$+ \int_{\bar{S}^e}\bar{\boldsymbol{t}}^{(e)}\cdot\delta\dot{\mathbf{u}}^{(e)}\mathrm{d}\bar{S} = \int_{\bar{V}^e}\bar{\rho}^{(e)}\ddot{\mathbf{u}}^{(e)}\cdot\delta\dot{\mathbf{u}}^{(e)}\mathrm{d}\bar{V}$$
$$(12)$$

where $\bar{V}^e$ and $\bar{S}^e$ are the volume and surface of the element defined by the structural part of the atomic position vectors $\bar{\mathbf{r}}_I$, as illustrated in Fig. 3. $\bar{\varsigma}_I$ is defined on $\bar{V}^e$ and $\bar{S}^e$. $\bar{\varsigma}_I$ is the fraction of atom I that is attributed to element $\bar{V}^e$. For periodic and amorphous structures alike, $\bar{\varsigma}_I$ can be defined through $\bar{\varsigma}_I^e = \bar{\varphi}^e / \sum_{e=1}^{q}\bar{\varphi}^e$, with $\bar{\varphi}^e$ being the solid angle (3D) or angle (2D) subtended by an element and q being the number of elements connected to atom at $\mathbf{r}_I$. Note that the delineation of $\boldsymbol{f}_I^{\text{int}}$ and $\boldsymbol{f}_I^{\text{ext}}$ is relative to $\bar{V}^e$ with $\bar{\eta}$ as

$$\begin{cases} \boldsymbol{f}_I^{\text{int}} = \displaystyle\sum_{J \neq I}^{M}\bar{\eta}_{IJ}\boldsymbol{f}_{IJ}, \\ \boldsymbol{f}_I^{\text{ext}} = \displaystyle\sum_{j,(J \neq 1,2,\cdots M)}^{N}\boldsymbol{f}_{Ij} + \boldsymbol{f}_I^o \end{cases} \quad (13)$$

Here, $\bar{\eta}_{IJ}$ is the fraction of the atomic bond that is spatially within element $\bar{V}^e$. It pertains to the bond between atoms I and J that are both inside $\bar{V}^e$. In general, when atoms are randomly distributed (as in amorphous materials), $\bar{\eta}_{IJ}$ is determined by the dihedral angle of the element as a fraction of the sum of such angles

$(\leq 360^{o})$ of all elements associated with the particular bond. Specifically, $\bar{\eta}^e_{IJ} = \phi^e_{IJ} / \sum^q_{e=1} \phi^e_{IJ}$, with ϕ^e_{IJ} being the dihedral angle in element (e) associated with the bond between atoms I and I, and q being the number of elements connected to the bond.

The high-frequency term in the above equation is

$$\widehat{\boldsymbol{f}}_I = -\bar{\varsigma}_I m_I \ddot{\bar{\mathbf{u}}}_I \qquad (14)$$

The association of $\widehat{\boldsymbol{f}}_I$ with the external force $\boldsymbol{f}^{\text{ext}}_I$ in Eq. (12) rather than $\boldsymbol{f}^{\text{int}}_I$ may appear to be somewhat arbitrary at first glance. However, it is strictly required by Newton's third law and by the necessity of maintaining the balance of momentum at all size scales. It is also required by the stipulation that full work rate equivalence be maintained between the EC and the molecular system. Furthermore, it is the only treatment that allows consistent handling of internal, external, and inertial work rates between the explicitly resolved particle motion as perceived by the observer and an equivalent continuum representation based on the macroscopically perceived particle motion. In particular, we note that Newton's third law requires that the sum of forces internal to a system or a portion of a system vanish. Otherwise, the system or the portion of that system would accelerate by its own effects and create energy and momentum. Here, the high-frequency inertial force term $(\widehat{\boldsymbol{f}}_I)$ cannot be associated with the internal force because, in general

$$\sum^M_{I=1} \left(\boldsymbol{f}^{\text{int}}_I + \widehat{\boldsymbol{f}}_I\right) \neq \mathbf{0} \text{ and } \sum^M_{I=1} \bar{\mathbf{r}}_I \times \left(\boldsymbol{f}^{\text{int}}_I + \widehat{\boldsymbol{f}}_I\right) \neq \mathbf{0} \qquad (15)$$

The component equations resulting from Eq. (12) are

$$\begin{cases} -\displaystyle\int_{\bar{V}^e} \bar{\boldsymbol{\sigma}}^{(e)} : \delta\bar{\mathbf{D}}^{(e)} \mathrm{d}\bar{V} = \sum^M_{I=1} \boldsymbol{f}^{\text{int}}_I \cdot \delta\dot{\bar{\mathbf{u}}}_I \\[2em] \displaystyle\int_{\bar{S}^e} \bar{\boldsymbol{t}}^{(e)} \cdot \delta\dot{\bar{\mathbf{u}}}^{(e)} \mathrm{d}\bar{S} = \sum^{M_S}_{I=1} (1 - \kappa_I)\boldsymbol{f}^{\text{ext}}_I \cdot \delta\dot{\bar{\mathbf{u}}}_I \\[2em] \displaystyle\int_{\bar{V}^e} \left(\bar{\boldsymbol{b}}^{(e)} + \widehat{\boldsymbol{b}}^{(e)}\right) \cdot \delta\dot{\bar{\mathbf{u}}}^{(e)} \mathrm{d}\bar{V} = \sum^M_{I=1} \left(\kappa_I \boldsymbol{f}^{\text{ext}}_I + \widehat{\boldsymbol{f}}_I\right) \cdot \delta\dot{\bar{\mathbf{u}}}_I \\[2em] \displaystyle\int_{\bar{V}^e} \bar{\rho}^{(e)} \ddot{\bar{\mathbf{u}}}^{(e)} \cdot \delta\dot{\bar{\mathbf{u}}}^{(e)} \mathrm{d}\bar{V} = \sum^M_{I=1} \bar{\varsigma}_I m_I \ddot{\bar{\mathbf{u}}}_I \cdot \delta\dot{\bar{\mathbf{u}}}_I \end{cases} \qquad (16)$$

where $\bar{\varsigma}_I$ is defined relative to $\bar{V}^e$. It is important to note that the thermal velocity term in Eqs. (12) and (16) accounts for the effect of the inertial force associated with the thermal fluctuations of the atoms on structural motion. It acts like an "invisible" external force. Clearly, it is not associated with a neighboring (or "interacting") atom, since the neighboring atom can have totally different thermal velocity and thermal acceleration. The inertial forces of two atoms are not equal in magnitude and opposite in direction. As a matter of fact, no part of the thermal velocities of any two neighboring atoms can be regarded as being coupled or out of mutual interactions. The inertial force term cannot be treated together with the internal (interactive) forces or stress. Ultimately, this is one of the reasons why thermal motions of atoms do not give rise to a contribution in terms of atomic velocity to stress directly.

The continuum description of the structural deformation is obtained via

$$\delta\dot{\bar{\mathbf{u}}}^{(e)}(\bar{\mathbf{x}}) = \sum^M_{I=1} \bar{N}_I(\bar{\mathbf{x}})\delta\dot{\bar{\mathbf{u}}}_I \qquad (17)$$

where $\bar{\mathbf{x}}$ represents continuum positions inside $\bar{V}^{(e)}$, just like $\mathbf{x}$ represents positions inside $V^{(e)}$. $\bar{N}_I(\bar{\mathbf{x}})$ are defined using the structural part of the atomic positions $\bar{\mathbf{r}}_I$ over $\bar{V}^{(e)}$. The corre-

sponding gradient of the virtual velocity field is

$$\frac{\partial \delta \dot{\mathbf{u}}^{(e)}}{\partial \bar{\mathbf{x}}} = \sum_{I=1}^{M} \delta \dot{\mathbf{u}}_I \otimes \frac{\partial \bar{N}_I}{\partial \bar{\mathbf{x}}} = \sum_{I=1}^{M} \delta \dot{\mathbf{u}}_I \otimes \bar{\mathbf{B}}_I \quad (18)$$

The equations for the stress over $\bar{V}^e$ are

$$\int_{\bar{V}^e} \bar{\boldsymbol{\sigma}}^{(e)} \cdot \bar{\mathbf{B}}_I \mathrm{d}\bar{V} = -\boldsymbol{f}_I^{\text{int}} \quad (19)$$

To obtain the traction over the surface area $\bar{S}^e$ of $\bar{V}^e$, consider a surface element $\Delta \bar{S}^e \subset \bar{S}^e$ defined by L particles. The continuum virtual velocity over $\Delta \bar{S}$ is

$$\delta \dot{\mathbf{u}}^{(e)}(\bar{\mathbf{x}}) = \sum_{I=1}^{L} \bar{N}_I(\bar{\mathbf{x}}) \delta \dot{\mathbf{u}}_I \quad (20)$$

where $\bar{N}_I(\bar{\mathbf{x}})$ is the appropriate shape function over $\Delta \bar{S}$. The corresponding traction field is

$$\bar{\boldsymbol{t}}^{(e)}(\bar{\mathbf{x}}) = \sum_{J=1}^{L} \bar{N}_J(\bar{\mathbf{x}}) \bar{\boldsymbol{\lambda}}_J \quad (21)$$

where $\bar{\boldsymbol{\lambda}}_J$ are vector solutions of the linear system of equations in the form

$$\sum_{J=1}^{L} \bar{c}_{IJ} \bar{\boldsymbol{\lambda}}_J = \bar{\xi}_I (1 - \kappa_I) \boldsymbol{f}_I^{\text{ext}} \quad (22)$$

In the above equations, $\bar{c}_{IJ} = \int_{\Delta \bar{S}} \bar{N}_I(\bar{\mathbf{x}}) \bar{N}_J(\bar{\mathbf{x}}) \mathrm{d}\bar{S}$, with $I, J = 1, 2, \cdots L$. $\bar{\xi}_I$ is the fraction of $(1 - \kappa_I) \boldsymbol{f}_I^{\text{ext}}$ that can be attributed to $\Delta \bar{S}$, since $\Delta \bar{S}$ may be only a portion of $\bar{S}^e$ and particle I may be on the boundary of $\Delta \bar{S}$ (shared by the rest of $\bar{S}^e$). $\bar{\xi}_I$ can be defined through $\bar{\xi}_I^i = \left(\Delta \bar{S}\right)_I^i / \sum_{i=1}^{q} \left(\Delta \bar{S}\right)_I^i$, with q being

the number of surface areas connected to atom I.

The equations for the body force density $\bar{\boldsymbol{b}}^{(e)}$ resulting from the third equation in Eq. (16) are

$$\bar{\boldsymbol{b}}^{(e)}(\bar{\mathbf{x}}) = \sum_{J=1}^{M} \bar{N}_J(\bar{\mathbf{x}}) \bar{\boldsymbol{v}}_J \quad (23)$$

where $\bar{\boldsymbol{v}}_J$ are the vector solutions of

$$\sum_{J=1}^{M} \bar{\mathrm{d}}_{IJ} \bar{\boldsymbol{v}}_J = \kappa_I \boldsymbol{f}_I^{ext} \quad (24)$$

In the above relations, $\bar{\mathrm{d}}_{IJ} = \int_{\bar{V}^e} \bar{N}_I(\bar{\mathbf{x}}) \bar{N}_J(\bar{\mathbf{x}}) \mathrm{d}\bar{V}$, with $I, J = 1, 2, \cdots M$. Similarly, the thermal oscillation-induced "body force" density $\widehat{\boldsymbol{b}}^{(e)}$ are

$$\widehat{\boldsymbol{b}}^{(e)}(\bar{\mathbf{x}}) = \sum_{J=1}^{M} \bar{N}_J(\bar{\mathbf{x}}) \widehat{\boldsymbol{v}}_J \quad (25)$$

where $\widehat{\boldsymbol{v}}_J$ are the vector solutions of

$$\sum_{J=1}^{M} \bar{\mathrm{d}}_{IJ} \widehat{\boldsymbol{v}}_J = \widehat{\boldsymbol{f}}_I \quad (26)$$

The mass density for $\bar{V}^e$ is

$$\bar{\rho}^{(e)}(\bar{\mathbf{x}}) = \sum_{K=1}^{M} \bar{N}_K(\bar{\mathbf{x}}) \bar{\mathrm{g}}_K \quad (27)$$

where $\bar{\mathrm{g}}_K \quad (K = 1, 2, \cdots M)$ are solutions of

$$\sum_{K=1}^{M} \bar{\mathrm{g}}_K \bar{\chi}_{IK} = \bar{\varsigma}_I m_I \ddot{\mathbf{u}}_I \quad (28)$$

with $\bar{\chi}_{IK} = \int_{\bar{V}^e} \bar{N}_I(\bar{\mathbf{x}})\bar{N}_K(\bar{\mathbf{x}})\ddot{\mathbf{u}}^e \mathrm{d}\bar{V}$ and $\ddot{\mathbf{u}}^e = \sum_{I=1}^{M} \bar{N}_I(\bar{\mathbf{x}})\ddot{\mathbf{u}}_I$. Equation (28) and the requirement that $\bar{\rho}^{(e)}$ be independent of $\ddot{\mathbf{u}}_I$ yields

$$\sum_{K=1}^{M} \bar{\mathrm{d}}_{IK}\,\bar{g}_K = \bar{\varsigma}_I m_I, \quad (I = 1, 2, \cdots M) \tag{29}$$

The replacement of $\delta\dot{\mathbf{u}}$ in Eqs. (12) and (16) with the actual structural deformation part of the velocity $\dot{\mathbf{u}}$ yields

$$\sum_{I=1}^{M} \boldsymbol{f}_I^{\mathrm{int}} \cdot \dot{\mathbf{u}}_I + \sum_{I=1}^{M} \left(\kappa_I \boldsymbol{f}_I^{\mathrm{ext}} + \widehat{\boldsymbol{f}}_I \right) \cdot \dot{\mathbf{u}}_I$$
$$+ \sum_{I=1}^{M_S} (1 - \kappa_I) \boldsymbol{f}_I^{\mathrm{ext}} \cdot \dot{\mathbf{u}}_I = \frac{\mathrm{d}}{\mathrm{d}t} \sum_{I=1}^{M} \tfrac{1}{2} \bar{\varsigma}_I\, m_I \dot{\mathbf{u}}_I \cdot \dot{\mathbf{u}}_I$$
$$= -\int_{\bar{V}^e} \bar{\boldsymbol{\sigma}}^{(e)} : \bar{\mathbf{D}}^{(e)} \mathrm{d}\bar{V} + \int_{\bar{V}^e} \left(\bar{\boldsymbol{b}}^{(e)} + \widehat{\boldsymbol{b}}^{(e)} \right) \cdot \dot{\mathbf{u}}^{(e)} \mathrm{d}\bar{V}$$
$$+ \int_{\bar{S}^e} \bar{\boldsymbol{t}}^{(e)} \cdot \dot{\mathbf{u}}^{(e)} \mathrm{d}\bar{S} = \frac{\mathrm{d}}{\mathrm{d}t} \int_{\bar{V}^e} \frac{1}{2} \bar{\rho}^{(e)} \dot{\mathbf{u}}^{(e)} \cdot \dot{\mathbf{u}}^{(e)} \mathrm{d}\bar{V} \tag{30}$$

Direct term-to-term equivalence is maintained here, establishing conservation of energy and equivalence of work rates from the perspective of the macroscopic observer. The term associated with the thermal oscillations of atoms is

$$\sum_{I=1}^{M} \widehat{\boldsymbol{f}}_I \cdot \dot{\mathbf{u}}_I = \int_{\bar{V}^e} \widehat{\boldsymbol{b}}^{(e)} \cdot \dot{\mathbf{u}}^{(e)} \mathrm{d}\bar{V} \tag{31}$$

This term represents the coupling or rate of energy exchange between the structural mode of the deformation ($\dot{\mathbf{u}}_I$) and the thermal mode of the deformation ($\tilde{\mathbf{u}}_I$) as it appears to the macroscopic observer. A positive value of this term indicates energy input from the thermal mode into the mechanical mode. Such cases

arise, for example, in thermally driven deformations. Although the thermal force $\widehat{\boldsymbol{f}}_I$ is "invisible" to the macroscopic observer, its effect on structural deformation and, perhaps more importantly, the energy exchange the above term represents can be clearly measured and plays an important role in microscopic and macroscopic phenomena. Examples include thermoelastic dissipation, thermoplastic dissipation, electromagnetically driven heat generation and deformation, thermal shock, and deformation driven by temperature changes.

It is important to point out that the "macroscopic" representation of Eq. (30) differs from the regular continuum balance of energy relation in the form of

$$-\int_{\underline{V}^e} \underline{\boldsymbol{\sigma}}^{(e)} : \underline{\mathbf{D}}^{(e)} \mathrm{d}\underline{V} + \int_{\underline{V}^e} \underline{\boldsymbol{b}}^{(e)} \cdot \dot{\underline{\mathbf{u}}}^{(e)} \mathrm{d}\underline{V} + \int_{\underline{S}^e} \underline{\boldsymbol{t}}^{(e)} \cdot \dot{\underline{\mathbf{u}}}^{(e)} \mathrm{d}\underline{S}$$
$$= \frac{\mathrm{d}}{\mathrm{d}t} \int_{\underline{V}^e} \tfrac{1}{2}\, \underline{\rho}^{(e)} \dot{\underline{\mathbf{u}}}^{(e)} \cdot \dot{\underline{\mathbf{u}}}^{(e)} \mathrm{d}\underline{V} \tag{32}$$

Although this relation is quite similar in form to that in Eq. (30), they have somewhat different meanings, depending on the scale. The quantities in Eq. (32) (denoted by an underscore) are *phenomenological* quantities developed for approximate descriptions of the atomic counterparts in Eq. (30). They may not be based on strict, full equivalence of momentum, energy, work rates, and mass at the atomic level. Since they are higher-scale concepts with much fewer numbers of degrees of freedom (DOF), they do not provide resolution of atomic scale behavior as the quantities in Eq. (30) (denoted by a superimposed bar) do. The following correspondence can be outlined based on physical mechanisms, without necessarily implying equality (equality holds if all the atomic DOF are used in the continuum representation).

$$\int_{\underline{V}^e} \underline{\boldsymbol{\sigma}}^{(e)} : \underline{\mathbf{D}}^{(e)} \mathrm{d}\underline{V} \Leftrightarrow \int_{\bar{V}^e} \bar{\boldsymbol{\sigma}}^{(e)} : \bar{\mathbf{D}}^{(e)} \mathrm{d}\bar{V} + \int_{\bar{V}^e} \widehat{\boldsymbol{b}}^{(e)} \cdot \dot{\mathbf{u}}^{(e)} \mathrm{d}\bar{V}$$

$$= \sum_{I=1}^{M} \boldsymbol{f}_I^{\mathrm{int}} \cdot \dot{\mathbf{u}}_I + \sum_{I=1}^{M} \widehat{\boldsymbol{f}}_I \cdot \dot{\mathbf{u}}_I$$

$$\int_{\underline{V}^e} \underline{\boldsymbol{b}}^{(e)} \cdot \underline{\mathbf{u}}^{(e)} \mathrm{d}\underline{V} \Leftrightarrow \int_{\bar{V}^e} \bar{\boldsymbol{b}}^{(e)} \cdot \dot{\mathbf{u}}^{(e)} \mathrm{d}\bar{V}$$

$$= \sum_{I=1}^{M} \kappa_I \boldsymbol{f}_I^{\mathrm{ext}} \cdot \dot{\mathbf{u}}_I$$

$$\int_{\underline{V}^e} \underline{\boldsymbol{t}}^{(e)} \cdot \underline{\mathbf{u}}^{(e)} \mathrm{d}\underline{S} \Leftrightarrow \int_{\bar{S}^e} \bar{\boldsymbol{t}}^{(e)} \cdot \dot{\mathbf{u}}^{(e)} \mathrm{d}\bar{S}$$

$$= \sum_{I=1}^{M_S} (1 - \kappa_I) \boldsymbol{f}_I^{\mathrm{ext}} \cdot \dot{\mathbf{u}}_I$$

$$\int_{\underline{V}^e} \tfrac{1}{2} \underline{\rho}^{(e)} \cdot \underline{\mathbf{u}}^{(e)} \cdot \underline{\mathbf{u}}^{(e)} \mathrm{d}\underline{V} \Leftrightarrow \int_{\bar{V}^e} \tfrac{1}{2} \bar{\rho}^{(e)} \dot{\mathbf{u}}^{(e)} \cdot \dot{\mathbf{u}}^{(e)} \mathrm{d}\bar{V}$$

$$= \frac{\mathrm{d}}{\mathrm{d}t} \sum_{I=1}^{M} \tfrac{1}{2} \bar{\varsigma}_I \, m_I \dot{\mathbf{u}}_I \cdot \dot{\mathbf{u}}_I \tag{33}$$

Of particular interest is the identification of the high-frequency thermal coupling term $\int_{\bar{V}^e} \widehat{\boldsymbol{b}}^{(e)} \cdot \dot{\mathbf{u}}^{(e)} \mathrm{d}\bar{V} = \sum_{I=1}^{M} \widehat{\boldsymbol{f}}_I \cdot \dot{\mathbf{u}}_I$ with the stress work rate in the first correspondence (rather than with the body force term in the second correspondence) in the above table. This identification reflects the continuum phenomenological description of thermoelastic dissipation and thermoplastic dissipation through the stress work, instead of through a "body-force-like" term, such as that in Eq. (30). Although this continuum phenomenological treatment is convenient and allows material behavior to be described with various degrees of accuracy at different length and time scales, the theoretical analysis here shows that it is fundamentally incompatible with the requirement of full work rate and momentum equivalence between the continuum description and the atomic reality.

The form of such a treatment does not allow full momentum and work equivalence to be obtained, even if the model is assigned the same number of degrees of freedom as the discrete atomic system. From the viewpoint of multiscale material behavior characterization from the "ground up" through molecular dynamics simulations, this association of thermal dissipation and thermostructural coupling with stress work rate can be used to formulate proper higher-scale, lower-DOF, phenomenological constitutive laws. For example, it can be defined that

$$\int_{\bar{V}^e} \widehat{\boldsymbol{b}}^{(e)} \cdot \dot{\mathbf{u}}^{(e)} \mathrm{d}\bar{V} = \int_{\bar{V}^e} \widehat{\boldsymbol{\sigma}}^{(e)} : \bar{\mathbf{D}}^{(e)} \mathrm{d}\bar{V} \tag{34}$$

Therefore,

$$\int_{\bar{V}^e} \bar{\boldsymbol{\sigma}}^{(e)} : \bar{\mathbf{D}}^{(e)} \mathrm{d}\bar{V} + \int_{\bar{V}^e} \widehat{\boldsymbol{b}}^{(e)} \cdot \dot{\mathbf{u}}^{(e)} \mathrm{d}\bar{V} = \int_{\bar{V}^e} \widehat{\boldsymbol{\sigma}}^{(e)} : \bar{\mathbf{D}}^{(e)} \mathrm{d}\bar{V} \tag{35}$$

It must be pointed out that Eq. (34) does not give a unique definition for $\widehat{\boldsymbol{\sigma}}^{(e)}$. More importantly, it is not possible to choose $\widehat{\boldsymbol{\sigma}}^{(e)}$ such that $\widehat{\boldsymbol{\sigma}}^{(e)}$ can be made to satisfy the balance of momentum [Eq. (12) or (19)]. Furthermore, this phenomenological association of thermal dissipation with the stress work rate cannot be construed as to imply dependence of stress on thermal velocity.

2.3 Thermal Oscillations: Balance of Energy and Thermal Fields

The analysis above is carried out from the perspective of a higher-scale observer with focus on the structural part of the atomic deformation ($\dot{\mathbf{u}}_I$). We now focus our analysis on the thermal

part of the deformation ($\dot{\tilde{\mathbf{u}}}_I$), from the perspective of an observer moving at velocity $\dot{\bar{\mathbf{u}}}_I$ with full resolution for thermal motions.

Equation (10) and the principle of virtual work over $\bar{V}^e$ with respect to $\delta\dot{\tilde{\mathbf{u}}}_I$ yield (after replacement of $\delta\dot{\tilde{\mathbf{u}}}_I$ by $\dot{\tilde{\mathbf{u}}}_I$ in the end)

$$
\sum_{I=1}^{M} \boldsymbol{f}_I^{\text{int}} \cdot \dot{\tilde{\mathbf{u}}}_I + \sum_{I=1}^{M} \left(\kappa_I \boldsymbol{f}_I^{\text{ext}} + \breve{\boldsymbol{f}}_I \right) \cdot \dot{\tilde{\mathbf{u}}}_I
$$
$$
+ \sum_{I=1}^{M_S} (1 - \kappa_I) \boldsymbol{f}_I^{\text{ext}} \cdot \dot{\tilde{\mathbf{u}}}_I = \frac{\mathrm{d}}{\mathrm{d}t} \sum_{I=1}^{M} \tfrac{1}{2} \bar{\varsigma}_I m_I \dot{\tilde{\mathbf{u}}}_I \cdot \dot{\tilde{\mathbf{u}}}_I
$$
$$
= - \int_{\bar{V}^e} \bar{\boldsymbol{\sigma}}^{(e)} : \tilde{\mathbf{D}}^{(e)} \mathrm{d}\bar{V} + \int_{\bar{V}^e} \left(\bar{\boldsymbol{b}}^{(e)} + \breve{\boldsymbol{b}}^{(e)} \right) \cdot \dot{\tilde{\mathbf{u}}}^{(e)} \mathrm{d}\bar{V}
$$
$$
+ \int_{\bar{S}^e} \bar{\boldsymbol{t}}^{(e)} \cdot \dot{\tilde{\mathbf{u}}}^{(e)} \mathrm{d}\bar{S} = \frac{\mathrm{d}}{\mathrm{d}t} \int_{\bar{V}^e} \tfrac{1}{2} \bar{\rho}^{(e)} \dot{\tilde{\mathbf{u}}}^{(e)} \cdot \dot{\tilde{\mathbf{u}}}^{(e)} \mathrm{d}\bar{V}
$$

$$\tag{36}$$

In the above relation,

$$
\breve{\boldsymbol{f}}_I = -\bar{\varsigma}_I m_I \ddot{\tilde{\mathbf{u}}}_I \tag{37}
$$

Also, term-to-term equality is maintained and

$$
\tilde{\mathbf{D}}^{(e)} = \tfrac{1}{2} \left[\frac{\partial \dot{\tilde{\mathbf{u}}}^{(e)}}{\partial \bar{\mathbf{x}}} + \left(\frac{\partial \dot{\tilde{\mathbf{u}}}^{(e)}}{\partial \bar{\mathbf{x}}} \right)^T \right]
$$
$$
= \tfrac{1}{2} \sum_{I=1}^{M} \left(\dot{\tilde{\mathbf{u}}}_I \otimes \bar{\mathbf{B}}_I + \bar{\mathbf{B}}_I \otimes \dot{\tilde{\mathbf{u}}}_I \right)
\tag{38}
$$

where $\dot{\tilde{\mathbf{u}}}^{(e)}$ is defined over $\bar{V}^e$ through

$$
\delta\dot{\tilde{\mathbf{u}}}^{(e)}(\bar{\mathbf{x}}) = \sum_{I=1}^{M} \bar{N}_I(\bar{\mathbf{x}}) \delta\dot{\tilde{\mathbf{u}}}_I \tag{39}
$$

Also, $\breve{\boldsymbol{b}}^{(e)}$ is calculated through Eqs. (25) and (26) with $\widehat{\boldsymbol{b}}^{(e)}$, $\widehat{\boldsymbol{v}}_J$, and $\widehat{\boldsymbol{f}}_I$ being replaced by $\breve{\boldsymbol{b}}^{(e)}$, $\breve{\boldsymbol{v}}_J$, and $\breve{\boldsymbol{f}}_I$, respectively. $\int_{\bar{V}^e} \breve{\boldsymbol{b}}^{(e)} \cdot \dot{\tilde{\mathbf{u}}}^{(e)} \mathrm{d}\bar{V} =$

$\sum_{I=1}^{M} \breve{\boldsymbol{f}}_I \cdot \dot{\tilde{\mathbf{u}}}_I$ represents work coupling between the thermal mode of deformation and the structural mode of deformation as it appears to an observer moving with the structural velocity $\dot{\bar{\mathbf{u}}}_I$. Specifically, it is the rate of energy input into the thermal mode of atomic motion.

Equation (36) represents the balance of energy as it appears to the observer traveling with the structural velocity $\dot{\bar{\mathbf{u}}}_I$ of an atom in the discrete description or to an observer traveling with velocity $\dot{\bar{\mathbf{u}}}^{(e)}$ of the (continuumized) mass point occupying $\mathbf{x}$ at time t in the equivalent continuum description. This equation is the atomic description of the thermal process in a coupled thermomechanical deformation event. The continuum phenomenological characterization is

$$
\int_{\underline{V}^e} \underline{h}^{(e)} \mathrm{d}\underline{V} + \int_{\underline{S}^e} \underline{\mathbf{n}}^{(e)} \cdot \underline{\mathbf{q}}^{(e)} \mathrm{d}\underline{S} = \frac{\mathrm{d}}{\mathrm{d}t} \int_{\underline{V}^e} \underline{\rho}^{(e)} (e_T + e_S) \mathrm{d}V
$$

$$\tag{40}$$

where $\underline{h}^{(e)}$ is the rate of phenomenological density of the heat source (thermal energy generated in the continuum per unit volume and per unit time), $\underline{\mathbf{q}}^{(e)}$ is the phenomenological heat flux (thermal energy flowing across unit surface area per unit time), e_T is the density of the thermal energy or the part of the internal energy associated with the thermal velocity of atoms, and e_S is the density of the part of the internal energy associated with interatomic force interactions. Since Eq. (40) is phenomenological in nature and involves much fewer degrees of freedom than Eq. (36), full and direct equivalence between the atomic equation and the macroscopic phenomenological equation may not be established. The following correspondences can be outlined based on physical mechanisms, without necessarily implying equality (equality holds if all the atomic DOF are used in the continuum representation).

Heat source :

$$
\int_{\underline{V}^e} \underline{h}^{(e)} \mathrm{d}\underline{V} \Leftrightarrow \int_{\bar{V}^e} \left(\bar{\boldsymbol{b}}^{(e)} + \breve{\boldsymbol{b}}^{(e)} \right) \cdot \dot{\bar{\mathbf{u}}}^{(e)} \mathrm{d}\bar{V}
$$

$$
= \sum_{I=1}^{M} \left(\kappa_I \boldsymbol{f}_I^{\mathrm{ext}} + \breve{\boldsymbol{f}}_I \right) \cdot \dot{\bar{\mathbf{u}}}_I
$$

Heat flow :

$$
\int_{\underline{S}^e} \underline{\mathbf{n}}^{(e)} \cdot \underline{\mathbf{q}}^{(e)} \mathrm{d}\underline{S} \Leftrightarrow \int_{\bar{S}^e} \bar{\boldsymbol{t}}^{(e)} \cdot \dot{\bar{\mathbf{u}}}^{(e)} \mathrm{d}\bar{S}
$$

$$
= \sum_{I=1}^{M_S} (1 - \kappa_I) \boldsymbol{f}_I^{\mathrm{ext}} \cdot \dot{\bar{\mathbf{u}}}_I
$$

Thermal energy :

$$
\frac{\mathrm{d}}{\mathrm{d}t} \int_{\underline{V}^e} \rho^{(e)} e_T \mathrm{d}\underline{V} \Leftrightarrow \frac{\mathrm{d}}{\mathrm{d}t} \int_{\bar{V}^e} \tfrac{1}{2} \bar{\rho}^{(e)} \dot{\bar{\mathbf{u}}}^{(e)} \cdot \dot{\bar{\mathbf{u}}}^{(e)} \mathrm{d}\bar{V}
$$

$$
= \frac{\mathrm{d}}{\mathrm{d}t} \sum_{I=1}^{M} \tfrac{1}{2} \bar{\varsigma}_I m_I \dot{\bar{\mathbf{u}}}_I \cdot \dot{\bar{\mathbf{u}}}_I
$$

Structural energy :

$$
\frac{\mathrm{d}}{\mathrm{d}t} \int_{\underline{V}^e} \rho^{(e)} e_S \mathrm{d}\underline{V} \Leftrightarrow \int_{\bar{V}^e} \bar{\boldsymbol{\sigma}}^{(e)} : \tilde{\mathbf{D}}^{(e)} \mathrm{d}\bar{V}
$$

$$
= - \sum_{I=1}^{M} \boldsymbol{f}_I^{\mathrm{int}} \cdot \dot{\bar{\mathbf{u}}}_I
$$

$$(41)$$

Note that the Reynolds transport theorem [9] specifies that $\frac{\mathrm{d}}{\mathrm{d}t} \int_{V^e} \rho^{(e)} e_S \mathrm{d}\underline{V} = \int_{V^e} \rho^{(e)} \dot{e}_S \mathrm{d}\underline{V}$.

Equations (36) and (41) allow phenomenological forms of heat equations at various scales to be formed based on the results of MD calculations. Specifically, the second relation above can be used to obtain characterizations of the thermal behavior of materials. To this end, we define the temperature at an atomic position through

$$
\tfrac{1}{2} m_i \dot{\bar{\mathbf{u}}}_i \cdot \dot{\bar{\mathbf{u}}}_i = \tfrac{3}{2} k T_i \tag{42}
$$

where k is the Boltzmann constant. We note that the standard definition of the *av-*

erage temperature ($\bar{T}$) for several atoms is only given in the statistical sense over a volume $\bar{V}^{(e)}$ of a system with M atoms through $\sum_{I=1}^{M} \tfrac{1}{2} m_I \dot{\bar{\mathbf{u}}}_I \cdot \dot{\bar{\mathbf{u}}}_I = \tfrac{3}{2} k \sum_{I=1}^{M} T_I = \tfrac{3}{2} M k \bar{T}$. The extension of this definition to individual atoms here is consistent with the statistical interpretations of temperature for aggregates of atoms. The statistical consistency is in the sense that the temperature of an aggregate of atoms is the average of the temperatures of the individual atoms. Some may argue that thermal energy (therefore, temperature) can only be measured (primarily) at higher scales in a statistically averaged, phenomenological manner, and it is difficult to measure the temperature of individual atoms and, therefore, the concept of the temperature of an individual atom is difficult to justify. A new and different perspective can be offered here. The advancement in scanning tunneling microscopy (STM) and atomic force microscopy (AFM) has brought to reality the ability to resolve and manipulate the positions of individual atoms (see, e.g., Refs. [10,11]). The thermal motions of individual atoms play a significant role in such processes and can be analyzed. If the thermal velocity of an atom can be clearly defined, the kinetic energy (thermal energy) associated with it can be defined and quantified as well. The atomic temperature defined in Eq. (42) has relevance, application, and scientific justification for the nanoscience of individual atoms and small clusters of atoms. This extension of the definition of temperature to an individual atom allows thermal analyses to be carried out at the nanoscale. We also note that this definition fully lends itself to interpretations in a statistical sense for higher-scale systems. Under this condition, the temperature field inside $\bar{V}^e$ can be expressed as

$$
T^{(e)}(\bar{\mathbf{x}}) = \sum_{I=1}^{M} \bar{N}_I(\bar{\mathbf{x}}) T_I \tag{43}
$$

It is specifically noted that the concept of temperature, just like the concept of thermal ve-

locity, is inherently scale dependent. The equivalence of thermal energy at an arbitrary size scale of $\bar{V}^e$ allows specific the heat $c^{(e)}$ to be defined through

$$\bar{\rho}^{(e)} e_T = \bar{\rho}^{(e)} c^{(e)} T^{(e)} = \tfrac{1}{2}\, \bar{\rho}^{(e)}\, \dot{\tilde{\mathbf{u}}}^{(e)} \cdot \dot{\tilde{\mathbf{u}}}^{(e)} \quad (44)$$

The governing equation for the heat flux inside $\bar{V}^{(e)}$ is the local version of Eq. (40) in the form of

$$\frac{\partial}{\partial \bar{\mathbf{x}}} \cdot \mathbf{q}^{(e)} = \underline{\rho}^{(e)}\left(\dot{e}_T + \dot{e}_S\right) - \underline{h}^{(e)}$$
$$= \left(\bar{\rho}^{(e)}\, \dot{\tilde{\mathbf{u}}}^{(e)} \cdot \ddot{\tilde{\mathbf{u}}}^{(e)} + \bar{\boldsymbol{\sigma}}^{(e)} : \tilde{\mathbf{D}}^{(e)}\right) - \left(\bar{\boldsymbol{b}}^{(e)} + \breve{\boldsymbol{b}}^{(e)}\right) \cdot \dot{\tilde{\mathbf{u}}}^{(e)}$$
$$(45)$$

This equation and the boundary requirement that

$$\bar{\mathbf{n}}^{(e)} \cdot \mathbf{q}^{(e)} = \bar{\mathbf{t}}^{(e)} \cdot \dot{\tilde{\mathbf{u}}}^{(e)} \quad (46)$$

over $\bar{S}^{(e)}$ allows $\mathbf{q}^{(e)}$ to be uniquely determined. The determination of $\mathbf{q}^{(e)}$ at all times yields $\dot{\mathbf{q}}^{(e)}$.

The thermal fields of temperature, specific heat, and heat flux carry information about the intrinsic thermal constitutive behavior of the atomic system. They can be used to formulate phenomenological continuum constitutive descriptions of the thermal behavior of material systems using MD calculations. Proper forms of thermal constitutive relations should be chosen within the context of specific systems, time scale, size scale, and the conditions involved. To illustrate how this can be achieved, we recognize the wave nature of heat conduction at the atomic level and consider the commonly used phenomenological relation between heat flux and temperature gradient in the form of

$$\boldsymbol{\tau} \cdot \dot{\mathbf{q}}^{(e)} + \mathbf{q}^{(e)} = -\mathbf{K}^{(e)} \cdot \frac{\partial T^{(e)}}{\partial \bar{\mathbf{x}}} \quad (47)$$

where $\boldsymbol{\tau}$ is the tensor of relaxation times and $\mathbf{K}^{(e)}$ is the thermal conductivity. $\boldsymbol{\tau}$ is positive-definite and, for simplicity, can be taken as

isotropic, i.e., $\boldsymbol{\tau} = \tau \mathbf{I}$, with $\mathbf{I}$ being the second-order identity tensor. τ is positive, reflecting the fact that the speeds of thermal waves [12] through atomic structures are finite. $\mathbf{K}^{(e)}$ is also positive-definite, reflecting the fact that heat flows from high-temperature regions to low-temperature regions. Equation (47) leads to heat equations that are hyperbolic in nature, accounting for the fact that ultimately at the atomic level, the conduction of heat is the propagation of high-frequency mechanical (thermal oscillation) waves through the atomic structure. This is especially the case at short time scales in applications such as heating induced by fast laser pulses (see, e.g., Refs. [13,14]). At higher size and time scales, the wave nature of the thermal process is smeared out and diffusion characteristics dominate, since sufficient time is available for relaxation to fully occur. To state this alternatively, if the time scale of analysis is orders of magnitude longer than τ, a transition to the limiting case with $\tau \to 0$ is justified, resulting in a parabolic heat equation commonly used at higher scales.

The determinations of the relaxation time tensor $\boldsymbol{\tau}$ and thermal conductivity $\mathbf{K}^{(e)}$ may require two separate calculations. First, the determination of $\mathbf{K}^{(e)}$ should, preferably, be carried out under steady-state thermal conditions for which $\dot{\mathbf{q}}^{(e)} = \mathbf{0}$, obviating the need for knowledge of $\boldsymbol{\tau}$. After the conductivity is determined, Eq. (47) can then be used to determine $\boldsymbol{\tau}$, based on the results of at least one separate MD calculation involving transient thermal responses. This should involve the choice of the nine components of $\boldsymbol{\tau}$ through, for example, curve-fitting, for the best description of the MD data. Materials with symmetries have fewer numbers of independent components for $\boldsymbol{\tau}$ and $\mathbf{K}$.

The specific heat and the thermal conductivity defined here are not thermodynamic quantities. They are fully dynamic, instantaneous measures for the thermal behavior of atomic

systems at various size scales. These definitions do not reflect statistical averaging, which is an intrinsic thermodynamic concept. Rather, they are quantities describing the thermal behavior of atomic systems with explicit resolutions in time and in structure, yet reckoned in the forms of standard (statistical) specific heat and thermal conductivity so as to conform to the continuum heat equation. Naturally, these dynamic quantities show oscillations and dependence on size, atomic structure, and composition of lattice waves at the atomic level. It is reasonable to expect that as the size scale of analysis is increased and as proper spatial and temporal averages are taken, these quantities will approach the microscopically or macroscopically measured values. Such analyses constitute future development. The quantification and approach introduced here provides an alternative to statistical mechanics for reaching microscopic, mesoscopic, and macroscopic continuum scales from a discrete molecular dynamics framework.

3. TENSILE DEFORMATION OF A RECTANGULAR LATTICE

Although the solutions of dynamic deformations of atomic systems are, in general, complex and require numerical treatment, a simple example can be analyzed here to illustrate the perspectives that the novel thermomechanical equivalent continuum theory has brought about. Some of the insights obtained here are revealing in terms of the form of stress, scale dependence, and thermal-mechanical coupling.

Consider the uniform tension of a rectangular lattice under external forces f^{ext} in Fig. 4. For simplicity, we assume that the deformation is strictly uniaxial. Thus, all atomic displacements and velocities are in the horizontal direction. Furthermore, we assume that the defor-
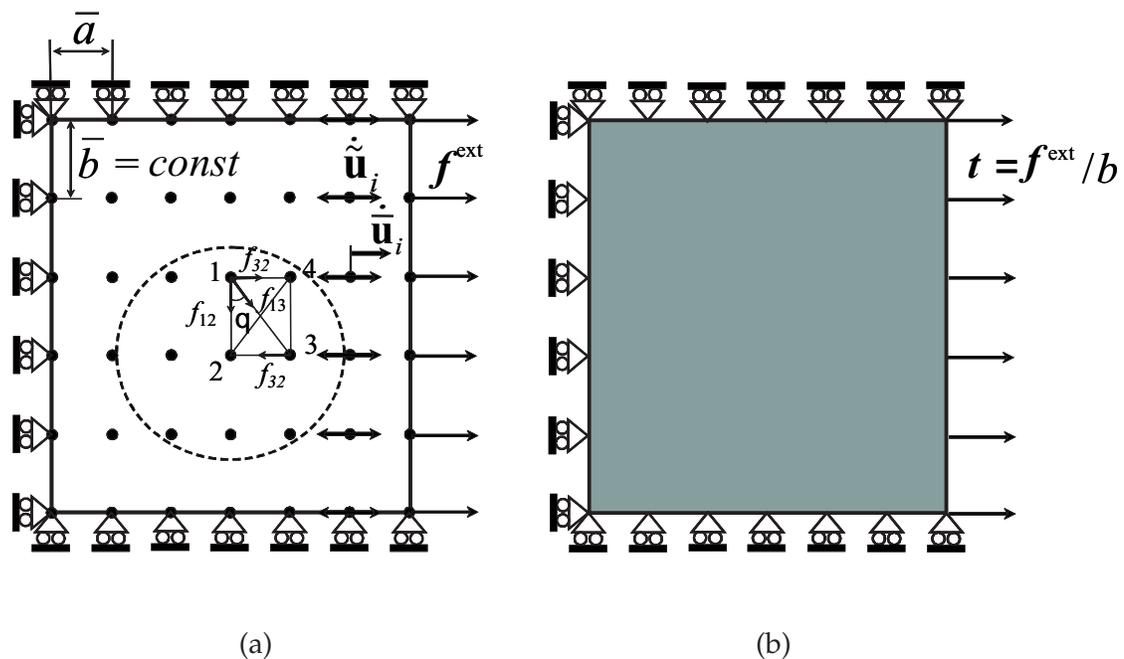

(a)   (b)

FIGURE 4. Tensile deformation of a lattice with thermal fluctuations under conditions of uniaxial strain

mation is uniform in the vertical direction; therefore, $\mathbf{u}_i(\mathbf{x}, t)$, $\bar{\mathbf{u}}_i(\bar{\mathbf{x}}, t)$ and $\tilde{\mathbf{u}}_i(\bar{\mathbf{x}}, t)$ are only functions of time and of $x(\bar{x})$, and are independent of $y(\bar{y})$ and $z(\bar{z})$. Although such a situation is idealized and cannot be easily brought about in the laboratory, it is perfectly allowed and has all the fundamental attributes of a dynamically deforming atomistic particle system, including the satisfaction of Eq. (4). It should also be pointed out at the outset of this analysis that although a time-resolved analysis is carried out at the scale of a unit lattice cell here, interpretation of the thermal behavior discussed has practical meaning primarily in the sense that the results be viewed as time averages over time. Full consistency of the thermal behavior with higher-scale characterizations occurs only when the size scale of analysis is much larger than what is the case here and when a proper time average is taken. However, this example allows the issue of a continuum representation of the MD system and the solution procedure to be illustrated.

As shown in Fig. 4, the deformed lattice has dimensions a and b in the horizontal and vertical directions, respectively. The material is homogeneous and the mass of each atom is m. For simplicity, we assume the cutoff radius R_c is such that $a < R_c < 2a$ and $b < R_c < 2b$, therefore, nonlocal interactions do not occur. Under the decomposition of Eq. (1), the atomic displacement has a uniform structural deformation part and a thermal oscillation part. Consequently

$$a(t) = \bar{a}(t) + \tilde{a}(t) \quad \text{and} \quad b(t) = \bar{b}(t) + \tilde{b}(t) \quad (48)$$

Since the deformation is assumed to be strictly one-dimensional, $b(t) = \bar{b}(t)$ and $\tilde{b}(t) = 0$. The calculation for the TMEC fields here uses 2D shape functions for rectangular elements (see, e.g., [15]). For the rectangular element defined by atoms 1, 2, 3, and 4 in Fig. 4, the shapes functions are

$$N_1(\mathbf{x}) = \left(1 - \frac{\mathrm{x} - \mathrm{x}_1}{a}\right)\frac{y - y_3}{b}$$

$$N_2(\mathbf{x}) = \left(1 - \frac{\mathrm{x} - \mathrm{x}_1}{a}\right)\left(1 - \frac{y - y_3}{b}\right)$$

$$N_3(\mathbf{x}) = \frac{\mathrm{x} - \mathrm{x}_1}{a}\left(1 - \frac{y - y_3}{b}\right)$$

$$N_4(\mathbf{x}) = \frac{\mathrm{x} - \mathrm{x}_1}{a}\frac{y - y_3}{b}$$

$$\bar{N}_1(\bar{\mathbf{x}}) = \left(1 - \frac{\bar{\mathrm{x}} - \bar{\mathrm{x}}_1}{\bar{a}}\right)\frac{\bar{y} - \bar{y}_3}{\bar{b}}$$

$$\bar{N}_2(\bar{\mathbf{x}}) = \left(1 - \frac{\bar{\mathrm{x}} - \bar{\mathrm{x}}_1}{\bar{a}}\right)\left(1 - \frac{\bar{y} - \bar{y}_3}{\bar{b}}\right)$$

$$\bar{N}_3(\bar{\mathbf{x}}) = \frac{\bar{\mathrm{x}} - \bar{\mathrm{x}}_1}{\bar{a}}\left(1 - \frac{\bar{y} - \bar{y}_3}{\bar{b}}\right)$$

$$\bar{N}_4(\bar{\mathbf{x}}) = \frac{\bar{\mathrm{x}} - \bar{\mathrm{x}}_1}{\bar{a}}\frac{\bar{y} - \bar{y}_3}{\bar{b}}$$

$$(49)$$

The interatomic forces vary with time [i.e., $f_{12} = f_{12}(a,b)$, $f_{13} = f_{13}(a,b)$, and $f_{32} = f_{32}(a,b)$] while they are uniform in the y direction since the deformation is uniform in that direction. All relevant continuum fields are summarized in Table 1. Both the results for the macroscopic TMEC representation and for the mechanical EC representation with full atomic displacement resolution are given. The stress, traction, body force, and deformation fields are consistent with the macroscopic expectations. It is important to note the difference and relationship between the stress representations at the macroscopic level and at the fully resolved atomic level. Both representations have similar forms. Although the stress (traction and body force, as well) at the fully resolved atomic level is evaluated relative to the instantaneous, true positions $\mathbf{r}_I$ of the atoms that define $V^{(e)}$, the stress (traction and body force, as well) at the macroscopic level is evaluated relative to the macroscopically perceived (structural) positions of the atoms $\bar{\mathbf{r}}_I$ that define $\bar{V}^{(e)}$. Both evaluations use the full instantaneous forces $\boldsymbol{f}_I$ on the atoms. Specifically, (see Eq. (50)).

TABLE 1. Mechanical and thermal quantities for a rectangular lattice in uniform tension

	Macroscopic resolution for $u_i = \bar{u}_i + \tilde{u}_i$ (Thermomechanical EC)	Full atomic resolution for u_i (Mechanical EC)
Stress	$\bar{\boldsymbol{\sigma}}^{(e)} =$ $\begin{pmatrix} \left(f_{32}+2f_{13}\sin\bar{\theta}\right)/\bar{b} & 0 \\ 0 & \left(f_{12}+2f_{13}\cos\bar{\theta}\right)/\bar{a} \end{pmatrix}$	$\boldsymbol{\sigma}^{(e)} =$ $\begin{pmatrix} \left(f_{32}+2f_{13}\sin\theta\right)/b & 0 \\ 0 & \left(f_{12}+2f_{13}\cos\theta\right)/a \end{pmatrix}$
Rate of deformation	$\bar{\mathbf{D}}=\begin{pmatrix} \dot{\bar{a}}/\bar{a} & 0 \\ 0 & \dot{\bar{b}}/\bar{b} \end{pmatrix}$ $\tilde{\mathbf{D}}=\begin{pmatrix} \dot{\tilde{a}}/\bar{a} & 0 \\ 0 & \dot{\tilde{b}}/\bar{b} \end{pmatrix}$,	$\mathbf{D}=\begin{pmatrix} \dot{a}/a & 0 \\ 0 & \dot{b}/b \end{pmatrix}$
Stress work rate	$\bar{\boldsymbol{\sigma}}^{(e)}:\bar{\mathbf{D}}^{(e)} = \frac{1}{\bar{a}\bar{b}}\left(f_{32}\dot{\bar{a}} + f_{12}\dot{\bar{b}} + 2f_{13}\dot{\bar{r}}\right)$ $\bar{r} = \sqrt{\bar{a}^2 + \bar{b}^2}$	$\boldsymbol{\sigma}^{(e)}:\mathbf{D}^{(e)} = \frac{1}{ab}\left(f_{32}\dot{a} + f_{12}\dot{b} + 2f_{13}\dot{r}\right)$ $r = \sqrt{a^2 + b^2}$
Traction	$\bar{\boldsymbol{t}} = -\left(f_1^{ext}/b\right)\mathbf{e}_x$ along side $1-2$ $\bar{\boldsymbol{t}} = \left(f_3^{ext}/\bar{b}\right)\mathbf{e}_x$ along side $3-4$ $\bar{\boldsymbol{t}} = \pm\left(f_{12} + 2f_{13}\cos\theta\right)\mathbf{e}_y/\bar{a}$ along sides $1-4$ and $2-3$	$\boldsymbol{t} = -\left(f_1^{ext}/b\right)\mathbf{e}_x$ along side $1-2$ $\boldsymbol{t} = \left(f_3^{ext}/b\right)\mathbf{e}_x$ along side $3-4$ $\boldsymbol{t} = \pm\left(f_{12} + 2f_{13}\cos\theta\right)\mathbf{e}_y/a$ along sides $1-4$ and $2-3$
Body force	$\bar{\boldsymbol{b}}^{(e)}(\bar{\mathrm{x}}) = \mathbf{0}$	$\boldsymbol{b}^{(e)}(\mathrm{x}) = \mathbf{0}$
Mass density	$\bar{\rho}^{(e)}(\bar{\mathrm{x}}) = \frac{m}{\bar{a}\bar{b}}$	$\rho^{(e)}(\mathrm{x}) = \frac{\mathrm{m}}{\mathrm{ab}}$
Inertial forces	$\widehat{\boldsymbol{b}}^{(e)}(\bar{\mathrm{x}}) = -\frac{m}{2\bar{a}\bar{b}}\left[\begin{array}{c}\left(2\ddot{\tilde{\mathbf{u}}}_1 - \ddot{\tilde{\mathbf{u}}}_3\right)\left(1 - \frac{\bar{\mathrm{x}}-\bar{\mathrm{x}}_1}{\bar{a}}\right) \\ + \left(2\ddot{\tilde{\mathbf{u}}}_3 - \ddot{\tilde{\mathbf{u}}}_1\right)\frac{\bar{\mathrm{x}}-\bar{\mathrm{x}}_1}{\bar{a}}\end{array}\right]$ $\breve{\boldsymbol{b}}^{(e)}(\bar{\mathrm{x}}) = -\frac{m}{2\bar{a}\bar{b}}\left[\begin{array}{c}\left(2\ddot{\bar{\mathbf{u}}}_1 - \ddot{\bar{\mathbf{u}}}_3\right)\left(1 - \frac{\bar{\mathrm{x}}-\bar{\mathrm{x}}_1}{\bar{a}}\right) \\ + \left(2\ddot{\bar{\mathbf{u}}}_3 - \ddot{\bar{\mathbf{u}}}_1\right)\frac{\bar{\mathrm{x}}-\bar{\mathrm{x}}_1}{\bar{a}}\end{array}\right]$	
Temperature	$T^{(e)}(\bar{\mathrm{x}}) = \frac{m}{3k}\left[\dot{\tilde{\mathbf{u}}}_1^2\left(1 - \frac{\bar{\mathrm{x}}-\bar{\mathrm{x}}_1}{\bar{a}}\right) + \dot{\tilde{\mathbf{u}}}_3^2\frac{\bar{\mathrm{x}}-\bar{\mathrm{x}}_1}{\bar{a}}\right]$	
Specific heat	$c^{(e)} = \frac{3k}{m}$	
Heat flux	$q_{\mathrm{x}}^{(e)}(\bar{\mathrm{x}}) =$ $\int\left[\begin{array}{c}\left(\bar{\rho}^{(e)}\dot{\mathbf{u}}^{(e)}\cdot\ddot{\mathbf{u}}^{(e)} + \bar{\boldsymbol{\sigma}}^{(e)}:\tilde{\mathbf{D}}^{(e)}\right) \\ -\left(\bar{\mathbf{b}}^{(e)} + \breve{\boldsymbol{b}}^{(e)}\right)\cdot\dot{\tilde{\mathbf{u}}}^{(e)}\end{array}\right]\mathrm{d}\bar{\mathrm{x}}$ with $q_{\mathrm{x}}^{(e)}(\bar{\mathrm{x}})\big|_{\bar{\mathrm{x}}=\bar{\mathrm{x}}_1} = -\frac{1}{b}\boldsymbol{f}_1^{\mathrm{ext}}\cdot\dot{\tilde{\mathbf{u}}}_1,\ q_{\mathrm{x}}^{(e)}(\bar{\mathrm{x}})\big|_{\bar{\mathrm{x}}=\bar{\mathrm{x}}_3}$ $= \frac{1}{b}\boldsymbol{f}_3^{\mathrm{ext}}\cdot\dot{\tilde{\mathbf{u}}}_3$ $\ddot{\mathbf{u}}^{(e)}(\mathrm{x}) = \ddot{\mathbf{u}}_1\left(1 - \frac{\bar{\mathrm{x}}-\bar{\mathrm{x}}_1}{\bar{a}}\right) + \ddot{\mathbf{u}}_3\frac{\bar{\mathrm{x}}-\bar{\mathrm{x}}_1}{\bar{a}}$	
Thermal conductivity	$\tau\dot{q}_{\mathrm{x}}^{(e)} + q_{\mathrm{x}}^{(e)} = -K_{\mathrm{xx}}^{(e)}\frac{\partial T^{(e)}}{\partial\bar{\mathrm{x}}}$ (steady-state calculation with $\dot{q}_{\mathrm{x}}^{(e)} = 0$)	
Relaxation time	$\tau\dot{q}_{\mathrm{x}}^{(e)} + q_{\mathrm{x}}^{(e)} = -K_{\mathrm{xx}}^{(e)}\frac{\partial T^{(e)}}{\partial\bar{\mathrm{x}}}$ (transient calculation with $\dot{q}_{\mathrm{x}}^{(e)} \neq 0$ after $K_{\mathrm{xx}}^{(e)}$ is determined)	

a) The atomic level uniaxial strain assumption implies that $\mathbf{u}_2 = \mathbf{u}_1$ and $\mathbf{u}_4 = \mathbf{u}_3$. $\mathrm{x}_2 = \mathrm{x}_1$ and $\mathrm{x}_4 = \mathrm{x}_3$ are the horizontal coordinates of the atoms in the element analyzed.

b) Here, $\kappa_I = 0$ and $\varsigma_I = 0.25$.

$$\boldsymbol{\sigma}^{(e)} = \begin{pmatrix} (f_{32} + 2f_{13}\sin\theta)/b & 0 \\ 0 & (f_{12} + 2f_{13}\cos\theta)/a \end{pmatrix} = \frac{1}{2V^{(e)}} \sum_{I}^{M} \sum_{J(\neq I)}^{M} \mathbf{r}_{IJ} \otimes (\eta_{IJ}\boldsymbol{f}_{IJ})$$

$$\bar{\boldsymbol{\sigma}}^{(e)} = \begin{pmatrix} (f_{32} + 2f_{13}\sin\bar\theta)/\bar{b} & 0 \\ 0 & (f_{12} + 2f_{13}\cos\bar\theta)/\bar{a} \end{pmatrix} = \frac{1}{2\bar{V}^{(e)}} \sum_{I}^{M} \sum_{J(\neq I)}^{M} \bar{\mathbf{r}}_{IJ} \otimes (\bar{\eta}_{IJ}\boldsymbol{f}_{IJ}) \quad (50)$$

For the volume element defined by atoms 1, 2, 3, and 4 in Fig. 4, $\eta_{IJ} = \bar{\eta}_{IJ} = 1/2$ for $\boldsymbol{f}_{12}$ and $\boldsymbol{f}_{32}$ since these forces are shared with neighboring cells. However, $\eta_{IJ} = \bar{\eta}_{IJ} = 1$ for $\boldsymbol{f}_{13}$ since this force is fully within the element. These coincide with the Cauchy stress expressions $\boldsymbol{\sigma}^{(e)}$ and $\bar{\boldsymbol{\sigma}}^{(e)}$ in Table 1.

The heat flux component in the x direction for the element analyzed in Table 1 is

$$q_x^{(e)}(\bar{\mathrm{x}}) = \int \left[\begin{array}{c} \left(\bar{\rho}^{(e)} \dot{\mathbf{u}}^{(e)} \cdot \ddot{\mathbf{u}}^{(e)} + \bar{\boldsymbol{\sigma}}^{(e)} : \tilde{\mathbf{D}}^{(e)} \right) \\ - \left(\bar{\boldsymbol{b}}^{(e)} + \breve{\boldsymbol{b}}^{(e)} \right) \cdot \dot{\mathbf{u}}^{(e)} \end{array} \right] d\bar{\mathrm{x}} \tag{51}$$

where the arbitrary constant resulting from the integration must be determined by Eq. (46) with takes the form of

$$q_x^{(e)}(\bar{\mathrm{x}})\Big|_{\bar{\mathrm{x}}=\bar{\mathrm{x}}_1} = -\frac{1}{\bar{b}} \boldsymbol{f}_1^{\text{ext}} \cdot \dot{\mathbf{u}}_1,$$

$$q_x^{(e)}(\bar{\mathrm{x}})\Big|_{\bar{\mathrm{x}}=\bar{\mathrm{x}}_3} = \frac{1}{\bar{b}} \boldsymbol{f}_3^{\text{ext}} \cdot \dot{\mathbf{u}}_3 \tag{52}$$

Clearly, $q_{\mathrm{x}}^{(e)}(\bar{\mathrm{x}})$ in Eq. (51) measures the flow rate of energy in the form of high-frequency mechanical waves through the element $\bar{V}^{(e)}$. This flow is apparently driven by the rate at which the thermal motion of the atoms on the boundary $\bar{S}^{(e)}$ can extract high-frequency mechanical work from or impart high-frequency mechanical work to its surroundings. Of course, the heat flow, so driven by the external excitation on the boundary $\bar{S}^{(e)}$, are effected through an imbalance inside $\bar{V}^{(e)}$ between the rate of change of the kinetic and potential energies associated with the thermal motions of the

atoms and the rate of work of the body force and inertial force over the thermal oscillations. To put it differently, heat flow across $\bar{V}^{(e)}$ is a manifestation, in the form of energy exchange, of the interaction of the high-frequency motion of $\bar{V}^{(e)}$, itself, with its surroundings.

At the macroscopic scale, a homogenous single crystal is expected to have a spatially uniform thermal conductivity $\mathbf{K}$. The mathematical forms of $T^{(e)}$, $c^{(e)}$, and $K_{\mathrm{xx}}^{(e)}$ in Table 1 for $\bar{V}^{(e)}$ do not necessarily conform to such macroscopic continuum phenomenological expectations, since they show spatial variations at the lattice level. The perspective obtained here is threefold.

First, explicit, time-resolved balance of momentum and conservation of energy is maintained in the TMEC analysis at all times. The result on the heat flux is quite illustrative. The significance of the results here should be more understood in the form of proper averages in time. For example, the temperature, specific heat, thermal conductivity, and relaxation time in Table 1 are more meaningful if interpreted as

$$\left\langle T^{(e)} \right\rangle = \frac{m}{3k} \left[\left\langle \dot{\mathbf{u}}_1^2 \right\rangle \left(1 - \frac{\bar{\mathrm{x}} - \bar{\mathrm{x}}_1}{\bar{a}} \right) + \left\langle \dot{\mathbf{u}}_3^2 \right\rangle \frac{\bar{\mathrm{x}} - \bar{\mathrm{x}}_1}{\bar{a}} \right]$$

$$\left\langle c^{(e)} \right\rangle = \frac{\left\langle \dot{\mathbf{u}}^{(e)} \cdot \dot{\mathbf{u}}^{(e)} \right\rangle}{2 \left\langle T^{(e)} \right\rangle} \quad \text{and}$$

$$\tau \left\langle \dot{q}_{\mathrm{x}}^{(e)} \right\rangle + \left\langle q_{\mathrm{x}}^{(e)} \right\rangle = - \left\langle K_{\mathrm{xx}}^{(e)} \right\rangle \left\langle \frac{\partial T^{(e)}}{\partial \bar{\mathrm{x}}} \right\rangle \tag{53}$$

where the angular brackets denote proper time averaging. As in experiments, the determination of $c^{(e)}$ and $K_{\mathrm{xx}}^{(e)}$ should be carried out when a steady state has been reached. The determina-

tion of τ, on the other hand, requires a transient impulse at one end.

Second, the atomic structure is explicitly accounted for. Under such conditions, the governing equations for the thermal process are then cast in the form of the macroscopic heat equation. The results at the nanoscopic scale naturally reflect the nature of the atomic structure. Consistency with higher length scale continuum expectations should emerge as one approaches higher scales. This entails the use of progressively large volume elements. In the process, the lattice-level variations of these quantities should average out and the long-range order should become apparent and dominant.

Third, thermal oscillations and structural deformations of atomic structures consist of waves of different frequencies (wavelengths). The wave spectrum is another source giving rise to time- and scale-dependence of responses. Macroscopic responses can only be observed when the analysis is carried out at spatial and temporal scales sufficient to represent all components of the lattice waves. The unit cell analysis above is at a scale well below many significant component wavelengths in the lattice. While this particular analysis at this particular scale shown in this example does not necessarily represent the higher-scale behavior, it indeed characterizes, rather faithfully and accurately, the atomic interactions at the lattice scale, albeit in a continuum form used at higher scales. The use of such a continuum form at all scales allows comparison, analysis of scaling effects, and transition from one scale to another.

4. CONCLUDING REMARKS

The thermomechanical equivalent continuum (TMEC) theory described here establishes, within the meaning of classical mechanics, the atomic origin of coupled thermomechanical de-

formation processes. It provides a framework for the formulation of coupled thermomechanical continuum descriptions of material behavior at any spatial and temporal scale "from the ground up," using molecular dynamics simulations. This theory is based on a decomposition of the atomic particle velocity into a relatively slower-varying structural deformation part and a high-frequency thermal oscillation part. The continuumization of the discrete molecular dynamics model is carried out with strict adherence to balance of momentum, balance of energy, and conservation of mass, in a fully dynamic and time-resolved manner. The establishment of equivalence between the discrete system and the continuum system follows the same approach used for the pure mechanical theory. This approach uses the dynamic principle of virtual work. Since the decomposition of atomic velocity into a structural deformation part and a thermal oscillation part is intrinsically dependent on both size and time scales, the development has followed a general framework of analysis, allowing scale-sensitive characterizations of both the structural deformation as it appears to a macroscopic observer and the thermal oscillation as it appear to an observer moving at the structural velocity of an atom. On one hand, balance of momentum at the structural level yields fields of stress, body force, traction, mass density, and deformation that maintain full dynamic equivalence between the discrete system and continuum system. This equivalence includes (i) preservation of linear and angular momenta; (ii) conservation of internal, external, and inertial work rates; and (iii) conservation of mass. On the other hand, balance of momentum in terms of the thermal motions yields the fields of heat flux and temperature. These quantities have been cast in a manner so as to conform to the continuum phenomenological equation for heat conduction and heat generation, allowing the specific heat, thermal conductivity, and re-

laxation time at different scales to be quantified. The coupling of the thermal equation of heat conduction and the mechanical equation of structural deformation, as phenomenologically known at higher continuum scales, occurs because the balance equations at the structural level and the thermal level are only two different forms of the same balance of momentum equation at the fully time-resolved atomic level. This coupling occurs through an inertial force term in each of the two equations [$\widehat{\boldsymbol{b}}^{(e)}$ in Eq. (30) and $\breve{\boldsymbol{b}}^{(e)}$ in Eq. (36)] induced by the other process. For the structural deformation equation, the inertial force term induced by thermal oscillations of atoms ($\widehat{\boldsymbol{b}}^{(e)}$) gives rise to the phenomenological dependence of deformation on temperature. This point can be seen from the first correspondence in Eq. (33). For the heat equation, the inertial force term induced by structural deformation ($\breve{\boldsymbol{b}}^{(e)}$) takes the phenomenological form of a heat source [see Eq. (41)]. Equations (30) and (36) represent conservation of energy as it appears to, respectively, the macroscopic observer (who sees $\dot{\bar{\mathbf{u}}}_i$) and the traveling observer (who sees $\dot{\check{\mathbf{u}}}_i$). Taken together, these two equations specify conservation of energy for the atomic system in the fully time-resolved sense. In summary, the TMEC theory developed here allows scale-dependent continuum descriptions of material behavior in the form of coupled thermomechanical processes of deformation and heat flow to be obtained from purely mechanical molecular dynamics simulations at the atomic level.

The framework here fully recognizes the spatial and temporal scale dependence of deformation. First, the choice of element $V^{(e)}$ is totally arbitrary, allowing size dependence of atomic behavior to be analyzed. Specifically, $V^{(e)}$ can be as small as the tetrahedron defined by four neighboring atoms, and as large as the whole system V. Length scale effects due to lattice spacing, thermal and structural wave lengths, and structural features such as voids and grains can be explicitly analyzed as the size of $V^{(e)}$ is varied. Such analyses, of course, carry a very significant computational cost.

The theoretical approach also fully admits the analysis of time scale influences. Specifically, the decomposition of atomic motion in Eq. (1) is highly dependent on time resolution. At the macroscopic time scale, high-frequency components of atomic oscillations are not explicitly resolvable and are, therefore, included in $\dot{\check{\mathbf{u}}}_i$. As the time resolution is increased, relatively lower-frequency components of atomic oscillations become explicitly resolved and are included in $\dot{\bar{\mathbf{u}}}_i$, causing $\dot{\check{\mathbf{u}}}_i$ to decrease. In the limit of an analysis with full resolution for atomic motion, $\dot{\check{\mathbf{u}}}_i = 0$ and $\dot{\mathbf{u}}_i = \dot{\bar{\mathbf{u}}}_i$. Consequently, the pure mechanical theory of equivalent continuum is recovered. Of course, temporal and spatial resolutions are often related and cannot be fully separated. Temporal resolutions are higher at small scales. For example, at the size scale of nanowires or electronic components, structural waves along the axial direction may need to be analyzed, causing the long wavelength (of the order of 1–2 nm) components of atomic motion to be included in $\dot{\bar{\mathbf{u}}}_i$. Such wave components may be regarded as thermal waves at the macroscopic level.

Finally, it is important to point out that the starting point of the theoretical development in this paper is molecular dynamics. The framework used here naturally inherits the assumptions and limitations of molecular dynamics. In particular, we note that the effect of free electrons on heat conduction in metals and alloys is not explicitly accounted for in standard MD models. Reflecting this characteristic of MD, the heat conduction analyzed in the TMEC theory developed in this paper concerns solely the contribution of atomic vibrations (or phonons) to thermal conductivity. In order to account for the contributions of free electrons (met-

als, alloys, and semiconductors; see, e.g., [16]), of electron/phonon interactions, and of bipolar carriers consisting of electron/hole pairs at high temperatures (semiconductors; see e.g., [17]) to thermal conductivity, modifications to the MD framework are required, if a framework within classical mechanics is to be used. This would constitute a significant extension of molecular dynamics, which is possible and, perhaps, worthwhile.

ACKNOWLEDGMENT

REFERENCES

1. Zhou, M., and McDowell, D. L., Equivalent continuum for dynamically deforming atomistic particle systems, *Philos. Mag. A* **82**:2547–2574, 2002.

2. Zhou, M., A new perspective of the atomic level virial stress: On continuum molecular system equivalence, *Proc. R. Soc. London, Ser. A* **459**:2347–2392, 2003.

3. Daw, M. S., and Baskes, M. I., Semiempirical, quantum mechanical calculation of hydrogen embrittlement in metals, *Phys. Rev. Lett.* **50**:1285–1288, 1983.

4. Baskes, M. I., Application of the embedded-atom method to covalent materials: a semiempirical potential for silicon, *Phys. Rev. Lett.* **59**:2666–2669, 1987.

5. Baskes, M. I., Nelson, J. S., and Wright, A. F., Semiempirical modified embedded-atom potentials for silicon and germanium, *Phys. Rev. B* **40**:6085–6100, 1989.

6. Carlsson, A. E., Beyond pair potentials in elemental transition metals and semiconductors, *Solid State Phys.* **43**:1–91, 1990.

7. Gavezzotti, A., Structure and intermolecular potentials in molecular crystals, *Modell. Simul. Mater. Sci. Eng.* **10**:R1–R29, 2002.

8. Born, M., and Huang, K., *Dynamical Theory of Crystal Lattices*, Clarendon Press, Oxford, 1988.

9. Malvern, L. E., *Introduction to the Mechanics of a Continuous Medium*, Prentice-Hall, Englewood Cliffs, N.J., 1969.

10. Alivisatos, A. P., Johnsson, K. P., Peng, X., Wilson, T. E., Lowth, C. J., Bruchez, M. P. J., and Schultz, P. G., Organization of "nanocrystal molecules" using DNA, *Nature* **382**:609–611, 1996.

11. Fishlock, T. W., Oral, A., Egdell, R. G., and Pethica, J. B., Manipulation of atoms across a surface at room temperature, *Nature* **404**:743–745, 2000.

12. Joseph, D. D., and Preziosi, L., Heat waves, *Rev. Mod. Phys.* **61**:41–73, 1989.

13. Hector, L. G. J., Kim, W.-S., and Oezisik, M. N., Hyperbolic heat conduction due to a mode locked laser pulse train, *Int. J. Eng. Sci.* **30**:1731–1744, 1992.

14. Kosinski W., and Frischmuth, K., Thermomechanical coupled waves in a nonlinear medium, *Wave Motion* **34**:131–141, 2001.

15. Reddy, J. N., *An Introduction to the Finite Element Method*, McGraw-Hill, N.Y., 1993.

16. Berman, R., *Thermal Conduction in Solids*, Oxford Studies in Physics, Clarendon Press, Oxford, 1976.

17. Bhandari C. M., and Rowe, D. M., *Thermal Conduction in Semiconductors*, Wiley Eastern Ltd., New Delhi, India, 1988.